

This is an Open Access document downloaded from ORCA, Cardiff University's institutional repository: <https://orca.cardiff.ac.uk/id/eprint/72810/>

This is the author's version of a work that was submitted to / accepted for publication.

Citation for final published version:

Attard, Gary Anthony and Brew, Ashley 2015. Cyclic voltammetry and oxygen reduction activity of the Pt{110}-(1×1) surface. *Journal of Electroanalytical Chemistry* 747 , pp. 123-129.
10.1016/j.jelechem.2015.04.017

Publishers page: <http://dx.doi.org/10.1016/j.jelechem.2015.04.017>

Please note:

Changes made as a result of publishing processes such as copy-editing, formatting and page numbers may not be reflected in this version. For the definitive version of this publication, please refer to the published source. You are advised to consult the publisher's version if you wish to cite this paper.

This version is being made available in accordance with publisher policies. See <http://orca.cf.ac.uk/policies.html> for usage policies. Copyright and moral rights for publications made available in ORCA are retained by the copyright holders.





Cyclic voltammetry and oxygen reduction activity of the Pt{110}-(1 × 1) surface



Gary A. Attard*, Ashley Brew

Cardiff Catalysis Institute, School of Chemistry, Cardiff University, Cardiff CF10 3AT, UK

ARTICLE INFO

Article history:

Received 19 November 2014

Received in revised form 21 March 2015

Accepted 14 April 2015

Available online 15 April 2015

Keywords:

Single crystal voltammetry

Oxygen reduction reaction

Surface reconstruction

ABSTRACT

A Pt{110}-(1 × 1) single-crystal electrode surface was created by flame annealing and cooling of the electrode in gaseous CO. For the first time, the voltammetry of this unreconstructed surface is reported using aqueous perchloric acid and sodium hydroxide electrolytes. The voltammetric response for Pt{110}-(1 × 1) produces marked differences when compared with the reconstructed, H₂- and N₂-cooled, disordered Pt{110}-(1 × 2) surface phases. Pt{110}-(1 × 1) exhibits as many as 6 individual peaks in the low potential region (0–0.25 V vs. Pd/H), a singular sharp oxidation peak at 0.95 V (Pd/H) corresponding to the electrosorption of oxide and almost zero current associated with OH formation between 0.6 V (Pd/H) and 0.9 V (Pd/H). Charge density curves indicate that the total charge passed between 0 V (Pd/H) and 1.5 V (Pd/H) to be almost identical for both the (1 × 1) and the disordered (1 × 2) phases in perchloric acid, sulphuric acid and sodium hydroxide electrolyte. The oxygen reduction reaction (ORR) activity of the (1 × 1) surface phase was also examined using rotating disc electrode voltammetry in the hanging meniscus configuration. The half-wave ORR peak potential was found to be ~30 mV more negative than for the disordered reconstructed surface. This leads to the conclusion that the activity of the unreconstructed basal planes of platinum towards the ORR follows the order {100} < {110} < {111} when $E_{1/2}$ is used as a measure of activity and that the higher activity usually ascribed to Pt{110} over Pt{111} is actually a manifestation of the disordered (1 × 2) surface phase in which step sites and defects promote ORR.

© 2015 The Authors. Published by Elsevier B.V. This is an open access article under the CC BY license (<http://creativecommons.org/licenses/by/4.0/>).

1. Introduction

In surface electrochemical studies, a reproducible electrochemical interphasial region is of the utmost importance in order to clarify structure–sensitivity relationships in electrocatalysis. This is because electrode reactions may be catalysed by different surface sites to varying degrees [1]. For the case of solid metal electrodes, these sites could include terraces, steps or kinks. If the electrode surface structure and composition are not reproducible, structure activity relationships and a true understanding of any surface electrode process will be impossible to deduce. However, even when electrodes are prepared in such a way that the condition of the surface is well-defined and the same surface structure and composition obtained every time an adsorption experiment is performed, it is not necessarily the case that correlations between reactivity and structure are unambiguous. For example, all (save for Ir{111}) of the basal planes of Pt, Ir and Au when clean may undergo surface reconstruction under

appropriate conditions [2,3] (the Pt{111} surface reconstructs only at high temperatures [4,5], or in the presence of saturated Pt vapour [6,7]). Hence, a fundamental question for electrocatalytic investigations would be how the reconstruction of a clean surface affects electrocatalytic activity? In the case of Pt{111} surfaces, the reconstructed state is not normally accessed under ambient electrochemical conditions. However, for Pt{100} differences in the reconstructive state of the electrode surface may be obtained by simply changing the ambient in which the electrode is prepared [8,9]. Will was the first to use platinum single crystal electrodes for electrochemical analysis in the 1960s [10]. Although preparing these crystals involved potential cycling to high potentials, a procedure Will acknowledged may change the surface structure, electrosorption features in the H_{UPD} region (0.05–0.3 V vs. RHE) in sulphuric acid electrolyte could be ascribed to particular adsorption sites using this procedure. The low potential H_{UPD} peak (0.12 V vs. RHE) was correctly assigned to the presence of {110} sites on the surface of polycrystalline platinum and the peak at more positive potentials (0.27 V vs RHE) to the presence of {100} sites. The flame annealing procedure used to prepare well-defined Pt electrode surfaces was first

* Corresponding author.

E-mail address: attard@cardiff.ac.uk (G.A. Attard).

reported by Clavilier and Durand leading to a great advance in our understanding of the relationships between surface structure and voltammetry [11]. In particular, the characteristic cyclic voltammetry of the clean and well-ordered Pt{111} surface in perchloric and sulphuric acid electrolytes was first reported [12]. It has since been shown that an intermediate cooling step in the flame annealing procedure may be instrumental in controlling surface reconstruction. A Pt{111}-(1 × 1) surface structure is obtainable using a cooling ambient of inert or reducing gases such as argon and hydrogen [13]. Similarly, cooling of a Pt{100} electrode after flame-annealing in a hydrogen ambient facilitates the formation of a Pt{100}-(1 × 1) surface structure [14]. In contrast, a reconstructed hex-R0.7° phase of Pt{100} is obtained when argon or nitrogen is employed as the cooling ambient with exclusion of all other gases [8]. Kolb et al. demonstrated that by flame annealing a Pt{110} electrode and cooling in a CO + N₂ atmosphere the (1 × 1) surface configuration would form whereas the Pt{110}-(1 × 2) “missing row” surface structure formed only when cooled in N₂ [13]. Markovic et al. using in situ surface X-ray diffraction (SXRD) also demonstrated that either the (1 × 2) or (1 × 1) surface atomic arrangements could be formed by using the same cooling environment (3% H₂ in Ar) but by controlling the gas phase quenching temperature [15]. In their work, the (1 × 1) phase was formed by rapid gas phase quenching at high temperature, whereas to form the (1 × 2) structure the crystal was allowed to cool before quenching. In Ref. [15] it was also reported that the (1 × 2) reconstruction would remain stable so long as potential excursions into the electrochemical oxide potential region were avoided. This was in accordance with previous ex situ LEED studies [16]. Astonishingly, in situ SXRD measurements by these workers also revealed that the (1 × 2) reconstruction remained unperturbed after the Pt{110} electrode had been exposed to carbon monoxide [15]. This points to a marked stability being bestowed upon the reconstructed phase by the electrochemical environment since under UHV conditions, adsorbed CO immediately lifts the clean surface reconstruction of Pt{110} [17]. In contrast, studies on stepped surfaces vicinal to Pt{110} suggested that CO displaces adsorbed hydrogen amounts slightly higher [18,19], but very close, to the theoretical (1 × 1) figure (147 μC cm⁻²) hence, suggesting an unreconstructed state after hydrogen cooling.

Bittner et al. [20] showed by electrochemical scanning tunnelling microscopy (EC-STM) that for a Pt{110} surface cooled in iodine, at very negative potentials (in H₂SO₄ electrolyte), the iodine desorbs and gives rise to an unreconstructed (1 × 1) surface with a surface topography consisting of small rectangular and isotropic terraces [20]. However, recent work by Rodriguez et al. [21] using voltammetry and in situ surface infra-red studies supported the notion of both the (1 × 1) and (1 × 2) surface phases of Pt{110} coexisting to different extents depending on the cooling environment. Later, we will show that this model is indeed consistent with the data presented in this study.

As mentioned earlier, many important electrocatalytic reactions carried out over platinum surfaces have been shown to be sensitive to the surface atomic arrangement. The oxygen reduction reaction (ORR) is one such reaction which shows not only increasing activity with surface step density but also different activities for the {100}, {110} and {111} basal planes. In some studies [22–26], Pt{110} exhibits high activity so that, when using the half-wave potential $E_{1/2}$ as a measure of ORR activity, the order of activity is {100} < {111} < {110}. Another study by Hoshi et al. has shown that, when using the current density at 0.9 V (vs. RHE) as a measure of activity, the {110} surface is approximately equal to {111} (0.59 vs. 0.60 mA cm⁻² respectively) but when using $E_{1/2}$ the order of activity is {100} < {110} < {111} [27].

Studies of the ORR usually utilise a H₂ or H₂/Ar cooling gas during the flame annealing procedure, producing the (1 × 1) unreconstructed surfaces of Pt{111} and {100}. As the Pt{110}-(1 × 1) surface requires stricter control over cooling conditions, it is likely that all previous studies have actually used a Pt{110}-(1 × 2) electrode or possibly a mixed (1 × 1)/(1 × 2) surface [15,21]. This means that structure–reactivity trends in the case of the basal planes of platinum for ORR may not be being compared on a strictly similar basis since one of the surfaces would actually be reconstructed/disordered whereas the other two would not:

Pt{100}-(1 × 1) < Pt{111}-(1 × 1) < disordered/Pt{110}-(1 × 2)?

No studies have looked at the ORR activity of the (1 × 1) unreconstructed Pt{110} surface, even though its voltammetry has been reported in sulphuric acid and has been shown to be quite distinct to that of the hydrogen-cooled surface [13]. In this paper we report the perchloric acid, sulphuric acid and sodium hydroxide voltammetry of the unreconstructed Pt{110} surface as well its ORR activity in perchloric acid. Also, we discuss this surface's stability towards potential cycling.

2. Materials and methods

A platinum {110} single-crystal electrode was prepared using the method of Clavilier [11]. The electrode was flame annealed and cooled in a CO or H₂ atmosphere and characterised in an electrochemical cell as described previously [28]. 0.1 mol dm⁻³ HClO₄, H₂SO₄ and NaOH electrolyte solutions were created by dilution of high purity reagents (HClO₄ 70% Suprapur[®] supplied by Merck, H₂SO₄ Aristar 95%, NaOH Sigma–Aldrich 99.9995%) in ultra-pure Milli-Q water with resistivity of >18.2 MΩ cm and used for the voltammetry reported herein. All electrolytes were sparged with high purity nitrogen for half an hour to remove dissolved carbon dioxide and oxygen prior to collection of each set of stationary voltammetry measurements. For ORR activity measurements, a Basi RDE-2 rotating disc electrode (RDE) was used for hydrodynamic control with a 0.1 mol dm⁻³ HClO₄ electrolyte saturated with ultra-pure oxygen (BOC 99.9999%) prepared by bubbling oxygen through the electrolyte for 30 min at 1 atm pressure. ORR measurements were collected in a hanging meniscus configuration [29].

A palladium hydride reference electrode was utilised in all experiments and was prepared by bubbling hydrogen over a palladium wire for half an hour, forming a stable palladium beta-hydride phase. Unless stated otherwise, all potentials are referenced to the Pd/H scale. For ORR activity measurements, the Pd/H reference electrode was placed in a luggin capillary filled with degassed 0.1 M aqueous perchloric acid. For both stationary and dynamic voltammetry, a platinum mesh was used as a counter electrode. For potential control, a CHI800 potentiostat interfaced with a PC using proprietary software was employed.

For CO adsorption, the Pt{110} crystal was flame annealed and cooled in CO gas, left in the CO atmosphere for 5 min, resulting in a CO covered surface. This was then transferred to the electrochemical cell protected by a droplet of the CO saturated electrolyte and contacted with the electrochemical cell electrolyte under potential control at 0 V (vs. PdH). After dispersing the excess CO by bubbling with argon, a positive going potential sweep from 0 V to 0.85 V was engaged to remove the CO adlayer leaving behind the pristine (1 × 1) surface. In the case of the preparation of the disordered Pt{110}-(1 × 2) phase, the CO cooling ambient was replaced by either pure hydrogen or pure nitrogen.

ORR activity was measured after voltammetric characterisation by transferring the Pt{110} electrode to the RDE cell, contacting

the electrolyte at a potential of 0 V and applying a positive potential sweep of 30 mVs^{-1} .

3. Results and discussion

3.1. Voltammetry

Fig. 1 shows cyclic voltammetry for an assumed Pt{110}-(1×1) single crystal electrode surface in aqueous 0.1 M sulphuric acid that was obtained by flame annealing and cooling in a CO ambient. Similarities in voltammetric response to Kolb et al. [13] can be seen here, namely the presence of a shoulder peak at 0.123 V which is not present in the voltammetry of the H_2 cooled Pt{110} surface. Although the peaks at $\sim 0.1 \text{ V}$ are larger for the CO-cooled electrode than for the hydrogen-cooled phase, the total charge passed in this region is approximately equal for both surfaces, $204 \mu\text{C cm}^{-2}$ for the hydrogen-cooled vs. $210 \mu\text{C cm}^{-2}$ for the CO-cooled (1×1) surface. Kolb and co-workers reported higher values of $\sim 275 \mu\text{C cm}^{-2}$ for the (1×1) surface after CO + N_2 cooling. Our results agree more closely to those achieved by Markovic et al., who also obtained sharper peaks for the (1×1) surface [15] and obtained approximately equal charges for the (1×1) and (1×2) surfaces of $\sim 180 \mu\text{C cm}^{-2}$ [30] in the low potential electroadsorption region.

Fig. 1 also shows the electrooxidation peak at $\sim 1 \text{ V}$ (ascribable to oxide formation) to be larger and sharper for the (1×1) phase compared to the hydrogen-cooled surface, implying a higher level of surface order for the (1×1) surface. This is also shown by the lower level of defect electroadsorption peaks for the (1×1) surface at around 0.8 V. The total charge passed between 0 and 1.5 V is approximately equal for both surfaces.

The voltammetry of the (1×1) surface in perchloric acid is shown in Fig. 2(a). The first scan shows oxidation of the CO adlayer ($\sim 96\%$ of charge in region 0–0.3 V blocked) to occur at 0.63 V. After removal of this adlayer, subsequent scans show peaks in the low potential region that are very different to those of the hydrogen-cooled and nitrogen-cooled surfaces (a direct comparison between all surfaces is shown in Fig. 2(b)). As many as 6 peaks are seen in Fig. 2(a) between 0 and 0.3 V in perchloric acid. The largest peak (P1) occurs at 0.09 V and has a shoulder (P2), which in some cases appears as a distinct peak, at 0.10 V. There is another pair of smaller peaks at slightly higher potentials, 0.135 V (P3) and 0.145 V (P4), and a final pair of peaks at 0.18 V (P5) and 0.20 V (P6). We performed peak fitting on the Pt{110}-(1×1) perchloric

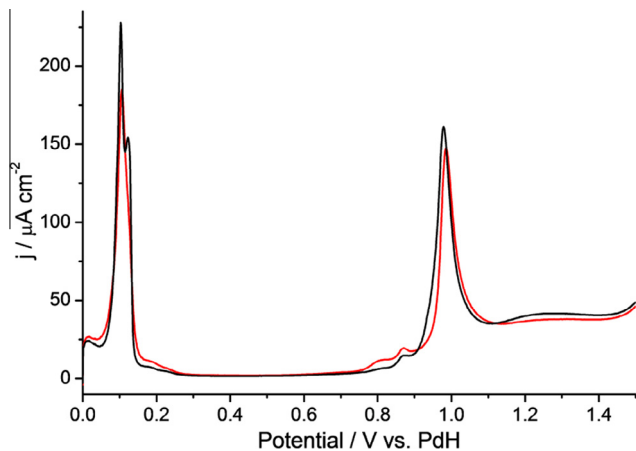


Fig. 1. Voltammetry of the hydrogen cooled Pt{110} surface (red) and the CO cooled Pt{110}-(1×1) surface (black) in $0.1 \text{ mol dm}^{-3} \text{ H}_2\text{SO}_4$. Sweep rate = 50 mV s^{-1} . (For interpretation of the references to colour in this figure legend, the reader is referred to the web version of this article.)

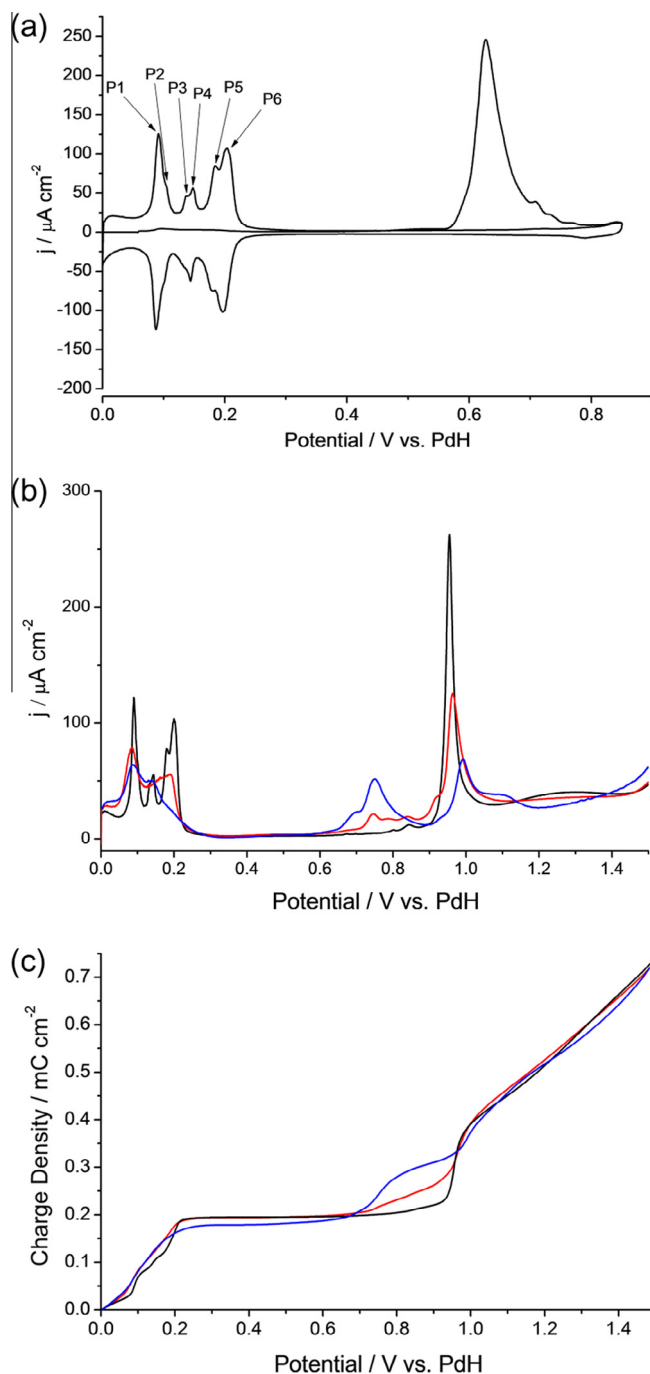


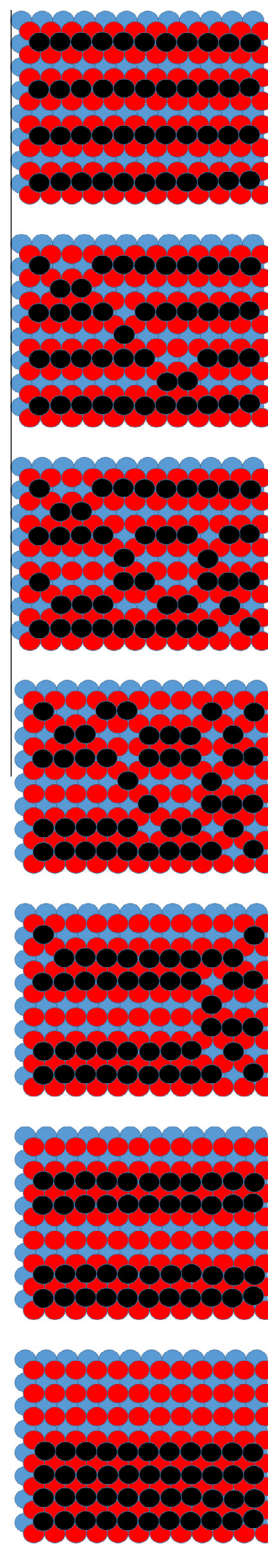
Fig. 2. (a) CO stripping voltammetry of the CO cooled Pt{110}-(1×1) electrode in $0.1 \text{ mol dm}^{-3} \text{ HClO}_4$. Sweep rate = 50 mV s^{-1} . (b) Voltammetry of the hydrogen-cooled Pt{110} surface (red), nitrogen-cooled Pt{110} (blue) and the CO cooled Pt{110}-(1×1) surface (black) in $0.1 \text{ mol dm}^{-3} \text{ HClO}_4$. Sweep rate = 50 mV s^{-1} . (c) Charge density vs. potential for the (1×1), black, hydrogen-cooled, red, and nitrogen-cooled, blue, voltammetry shown in (b). (For interpretation of the references to colour in this figure legend, the reader is referred to the web version of this article.)

acid voltammetry in the 0.05–0.25 V potential range in order to elucidate the approximate charge associated with each of these peak processes. From this analysis P1 was found to have a charge of $\sim 32 \mu\text{C cm}^{-2}$, P2 a charge of $\sim 5 \mu\text{C cm}^{-2}$, P3 $\sim 5.5 \mu\text{C cm}^{-2}$, P4 $\sim 6.5 \mu\text{C cm}^{-2}$, P5 $\sim 25 \mu\text{C cm}^{-2}$ and P6 a charge of $\sim 43 \mu\text{C cm}^{-2}$. The voltammetry reveals an extra $20 \mu\text{C cm}^{-2}$ to be associated with H_{ads} electroadsorbed negative of 50 mV (vs. Pd/H), bringing

the total to $\sim 137 \mu\text{C cm}^{-2}$. The remaining charge of $\sim 60 \mu\text{C cm}^{-2}$ was associated with background current that could not be ascribed to peak processes listed above, reaching the total of $\sim 200 \mu\text{C cm}^{-2}$ that is seen between 0 and 0.25 V in Fig. 2(c). Since a theoretical charge of only $147 \mu\text{C cm}^{-2}$ is predicted for a perfect (1×1) surface and it is unlikely that this surface is defective based on its CV response, it is speculated that a second species is coadsorbed. As postulated using CO charge displacement studies [18,19], we suggest that water splitting to form OH is the likeliest candidate here and that a PZTC value of around 0.18 V (Pd/H) is expected (potential where $147 \mu\text{C cm}^{-2}$ of H_{upd} charge is passed). This value would be close to the PZTC of a hydrogen-cooled Pt{110} electrode [31].

Despite the multitude of peaks in this low potential range, Fig. 2(b) shows a single sharp oxidation peak at ~ 0.95 V for the (1×1) surface. The (1×1) surface's combination of a very sharp oxidation peak at 0.95 V and a multiplicity of peaks below 0.3 V implies an atomically perfect (1×1) surface with multiple and distinct energetic states in which $H_{\text{ads}}/\text{OH}_{\text{ads}}$ can coadsorb as a function of potential. In fact we assert that only long range order giving rise to large domains of Pt{110}– (1×1) can generate such a multitude of sharp narrow peaks on Pt{110} in a similar manner to the so-called “butterfly” peaks on Pt{111} reflecting long range order being present in the surface.

In contrast, the hydrogen-cooled electrode voltammetric response exhibits only 2 peaks between 0 and 0.3 V, one at 0.09 V and another broad feature at 0.22 V (see red Fig. 2(b)). This surface also exhibits an oxidation peak at 0.95 V which is half the height of the peak for the (1×1) surface and shows higher current responses for electrosorption of OH/oxide at defects between 0.6 and 0.9 V. We presume that (1×1) domains are actually present on this hydrogen-cooled electrode but that they are of lower surface density resulting in a 50% decrease in the magnitude of the $\{110\}$ – (1×1) 0.95 V peak. In a further manifestation of how the cooling environment influences the voltammetric response of a flame-annealed Pt{110} electrode, when nitrogen cooling is employed, the extent of 1×1 surface order (as signified by the intensity of the oxide electrosorption peak at 0.95 V) is reduced still further and much greater peak intensity due to adsorption at defects (0.6–0.9 V) observed. It is noted that according to Kolb and co-workers [13], such treatment results in the generation of a reconstructed (1×2) phase (indeed according to Attard et al. the same is also true of Pt{100} whereby a reconstructed hex $R0.7^\circ$ phase forms [8]). It should also be noted that the adsorption at “defects” occurs at rather negative potentials. Unpublished work from our group studying correlations between peak potential of electrosorbed OH species and step density/symmetry have shown that the small peaks between 0.84 and 0.87 V correspond to OH adsorbing at $(111) \times (100)$ and $(100) \times (110)$ linear steps respectively. For the nitrogen-cooled sample, the large OH adsorption peak at 0.74 V is normally associated with the potential range ascribable to OH adsorption at $\{111\}$ terraces rather than steps or kinks [32]. If this is the case, it would suggest that residual $\{111\}$ adsorption sites, possibly from the (1×2) reconstructed phase, are still present under electrochemical conditions for the nitrogen-cooled surface. Returning to the H_{upd} potential range, it is interesting that there is an exact correlation between the magnitude of the 0.2 V electrosorption feature and the oxide electrosorption peak situated between 0.95 and 1.0 V. Hence, as mentioned earlier, this 0.2 V peak profile must be arising from the degree of long range (1×1) order present at the surface. There is also an interesting lowering in intensity and broadening of the 0.09 V peak as surface disorder increases. In order to visualise these changes, a schematic model of what might be happening as cooling environment is changed is shown in Scheme 1. Here, we start with a pristine, reconstructed Pt{110}– (1×2) phase. In order to form



Scheme 1. An ordered (110) – (1×2) , top, and (110) – (1×1) surface, bottom. The centre illustrations show disordered arrangements that are closer to (1×2) in nature near the top and close to (1×1) near the bottom.

regions of (1×1) (constituting an increase in the disorder of the (1×2) phase) surface diffusion perpendicular to the close packed atomic rows is envisaged. If this process continues, eventually the surface will transform continuously from a (1×2) to a (1×1) phase, especially if thermalizing of the surface is allowed (flame annealing). However, the thermodynamically stable clean

surface of Pt{110} under UHV conditions is the (1×2) phase. Since chemical interactions between a Pt surface and molecular nitrogen are negligible, cooling in a nitrogen ambient should still result in a (1×2) phase being preserved (the same as found for Pt{100} hex $R0.7^\circ$ [8]). However, as the interaction of Pt with the gas ambient increases, it is expected that a new thermodynamically stable state should result involving a lifting of the 1×2 reconstruction (as reported in UHV). Hence, since CO is a more strongly interacting chemisorbate compared to hydrogen, the extent of surface reconstruction lifting should be greatest with CO-cooled samples with hydrogen-cooled surfaces displaying an intermediate behaviour between that of CO-cooled and N_2 -cooled substrates. Therefore, according to Scheme 1, we place the nitrogen-cooled electrode close to the top (more (1×2) reconstructed), hydrogen-cooled electrodes somewhere in the middle and CO-cooled samples close to the perfect (1×1) phase. This idea of “mixed” $(1 \times 2)/(1 \times 1)$ surface structure is in accordance with previous IR studies of CO adsorption on Pt{110} by Paramaconi and coworkers [21]. By suitable peak deconvolution of the oxide electroadsorption region in particular, it may be possible to quantify the extent of $(1 \times 1)/(1 \times 2)$ mixing. In fact, we speculate that the very low potential for electrochemical oxide formation in the case of the nitrogen-cooled sample is consistent with electroadsorption of OH at the highly unsaturated, close-packed chains of Pt atoms formed in the (1×2) -Pt{110} phase. These atomic sites should be highly oxophilic compared to even kink and step sites due to their very low surface coordination and are predicted to display unusual electrocatalytic behaviour towards electrooxidation reactions. Hence, we propose that the magnitude of the 0.74 V OH peak on Pt{110} is proportional to the extent of (1×2) surface reconstruction present under electrochemical conditions. These ideas will be examined further in future work.

Feliu et al. have speculatively ascribed the broad feature at 0.22 V formed from hydrogen-cooling to co-adsorption of hydrogen and OH species [33]. The $105 \mu\text{C cm}^{-2}$ charge of the low potential peak in their work was assigned solely to H_{ads} formation and the $90 \mu\text{C cm}^{-2}$ charge of the broad feature close to 0.2 V was assigned to coadsorption of adsorbed OH based on the value of the PZTC of the surface. The total charge of almost $200 \mu\text{C cm}^{-2}$ for the two peaks is the same as the charge obtained by ourselves and shown in Fig. 2(c).

The many peaks that we observe below 0.3 V for the (1×1) surface suggest also that that co-adsorption of H and OH is occurring. If P1, P3 and P5 are thought to be H_{ads} and P2, P4 and P6 thought to be OH_{ads} , this would imply that between 0.09 and 0.2 V the surface is covered by a mixed $H_{\text{ads}}/OH_{\text{ads}}$ overlayer. With changing potential, the ratio of H to OH changes as new overlayer structures are preferred. It may be further concluded that the ordered (1×1) surface only has a couple of distinct stable overlayer structures, and that the peaks between 0 and 0.3 V correspond to transformation between these structures. Further theoretical studies are required to confirm this hypothesis. In all of these speculations, the existence of an OH species at such negative potentials is a vexatious and difficult concept. However, recent work supporting water splitting and surface pH values differing from the bulk might suggest a possible resolution of this conundrum [34].

In light of this idea some general conclusions can also be made about the disordered (1×2) surface as this surface exhibits current responses in the same potential range as the (1×1) surface. We ascribe the broad feature of the disordered (1×2) surface, between 0.1 and 0.25 V, to a changing $H_{\text{ads}}/OH_{\text{ads}}$ over-layer, in a similar fashion to the (1×1) surface described above. P2–P6 in the voltammetry of (1×1) may also be occurring in the voltammetry of the disordered (1×2) surface, but to a lesser extent, and combined with H_{ads} on the short (111) terraces of the (1×2) structure. The loss of long range order in the (1×1) phase would

be consistent with both a broadening and decrease in intensity of electroadsorption features similar to when the H UPD region of Pt{hkl} surfaces is strongly modified after potential cycles to high positive potentials [35].

Fig. 2(c) shows how charge varies as a function of potential for the voltammograms depicted in Fig. 2(b). These have not been adjusted for the PZTC as this value has not been determined for the (1×1) surface as yet. Between 0 and 1.5 V the same total charge is passed for all surfaces. Also, the charge passed between 0 and 0.3 V is the same ($\sim 200 \mu\text{C cm}^{-2}$) for the disordered (1×2) and (1×1) surfaces and is equal to the charge passed in this potential range in sulphuric acid. The charge passed in this range is greater than the theoretical charge that should be passed for pure H_{ads} formation at every surface atom, $147 \mu\text{C cm}^{-2}$, as has been noted in a previous study [30]. Therefore the total charge of $200 \mu\text{C cm}^{-2}$ must come from a combination of H_{ads} and OH_{ads} since voltammetry suggests strongly that the surface is atomically smooth (negligible OH/oxide adsorption at defect sites) as suggested earlier.

Next, the stability of the Pt{110}– (1×1) surface was tested using potential window opening to high positive potentials in perchloric acid and the results of this procedure are shown in Fig. 3(a)–(c). With an upper potential limit of 0.9 V (Fig. 3(a)) the voltammetry of the (1×1) surface shows small but noticeable changes during five potential cycles. The peaks between 0 and 0.3 V very gradually diminish with cycling and current density in the troughs between the peaks increases at the same rate. This implies instability of the (1×1) surface even when the potential is set so that surface oxide is not formed. Nonetheless, 0.9 V does represent a rather positive potential for surface stability compared to all other Pt{hkl} electrodes save for Pt{111}. When the upper potential limit is increased to 0.95 V (Fig. 3(b)), greater changes are seen in the voltammetry with cycling. At this potential limit surface oxide formation begins but is not completed. Within 5 potential cycles the voltammetry changes from that characteristic of the (1×1) surface and approaches the voltammetry usually observed after cooling in hydrogen (ascribable to the presence of disordered (1×2) domains). With an upper potential limit of 1 V (Fig. 3(c)), even after 1 cycle the voltammetry has changed dramatically and irreversibly. After 5 cycles within this potential limit, the voltammetry between 0 and 0.3 V looks like the hydrogen cooled surface shown in Fig. 2(a), implying a $(1 \times 1) \rightarrow$ disordered (1×2) rearrangement after oxide formation and desorption (in Scheme 1 corresponding to a movement in the opposite direction discussed for nitrogen-, hydrogen- and CO-cooled electrodes).

The voltammetry of the CO- and H_2 -cooled surfaces was then tested in 0.1 M NaOH and the results are shown in Fig. 4(a). For Pt{110}– (1×1) , at high potentials voltammetric behaviour is similar to that found in perchloric and sulphuric acid whereby only limited electroadsorption peaks for adsorption of OH/oxide at defects is observed. A large peak associated with oxide formation is observed at 1 V. At more negative potentials, the (1×1) surface exhibits a pair of peaks that have greater intensity than the hydrogen-cooled surface. The main peak is located at 0.22 V and exhibits a distinct shoulder at 0.25 V. Fig. 4(b) illustrates the charge density for the two surfaces. Between 0 and 0.4 V, both (1×1) and hydrogen-cooled surfaces generate a charge of $\sim 230 \mu\text{C cm}^{-2}$. At ~ 0.7 V and above, surface defects of the hydrogen-cooled surface are responsible for its higher charge. The overall charge, between 0 and 1.5 V, for both surfaces is approximately equal, as was seen in both sulphuric and perchloric acid electrolytes.

3.2. Oxygen reduction reaction

The ORR activity of the Pt{110}– (1×1) , hydrogen- and nitrogen-cooled Pt{110} surface phases was tested using hanging

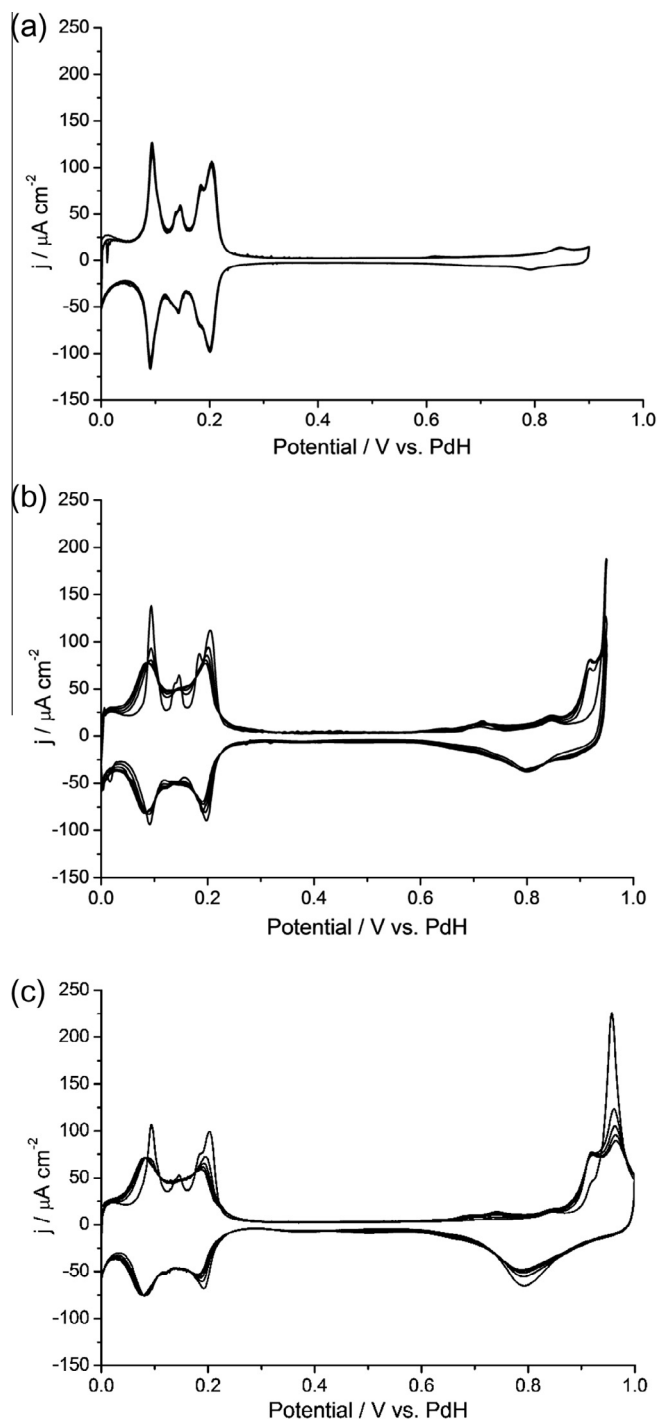


Fig. 3. Test of increasing potential limits on the voltammetry of the Pt{110}-(1 × 1) surface in 0.1 mol dm⁻³ HClO₄. (a) 0–0.9 V. (b) 0–0.95 V. (c) 0–1 V. 5 Cycles with sweep rate = 50 mV s⁻¹.

meniscus rotating disc voltammetry and the results are shown in Fig. 5. Oxygen reduction half wave potentials ($E_{1/2}$) of 0.795 V and 0.765 V for the hydrogen-cooled and (1 × 1) surfaces respectively are noted. These results demonstrate that the disordered (1 × 2) surface phase of the hydrogen-cooled electrode exhibits the greater activity towards ORR. When using the current density at 0.85 V as a measure of ORR activity, one observes the disordered Pt{110}-(1 × 2) surface to possess an even higher activity than the Pt{111} surface, ~1.1 mA cm⁻² vs. ~0.8 mA cm⁻² respectively. The

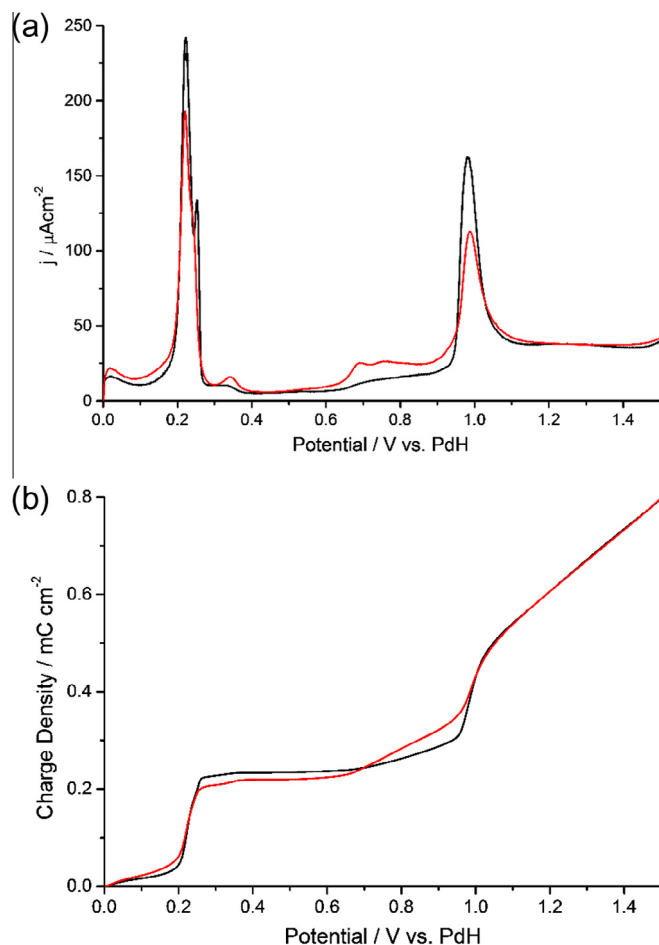


Fig. 4. Voltammetry of the hydrogen cooled Pt{110} surface (red) and the CO cooled Pt{110}-(1 × 1) surface (black) in 0.1 mol dm⁻³ NaOH. Sweep rate = 50 mV s⁻¹. (b) Charge density vs. potential for the (1 × 1) and hydrogen-cooled electrode voltammetry shown in (a). (For interpretation of the references to colour in this figure legend, the reader is referred to the web version of this article.)

current density at 0.85 V of the Pt{110}-(1 × 1) surface is ~0.8 mA cm⁻², a reduction of almost 30% in current compared to the hydrogen-cooled surface, bringing its activity in line with that of Pt{111}. Also shown in Fig. 5 is the ORR results for the nitrogen-cooled electrode. According to the voltammetric data this surface corresponds to the most “disordered” relative to the pristine (1 × 1) phase and we speculate, corresponds most closely to a reconstructed (1 × 2) phase. As expected, further disruption of the (1 × 1) terraces results in still greater enhancement in ORR activity compared to the hydrogen-cooled sample. Therefore, comparing the ORR activity of the (1 × 1) platinum basal planes in their *unreconstructed state* results in the following order of activity:

$$\{1\ 0\ 0\} < \{1\ 1\ 0\} < \{1\ 1\ 1\}$$

It has been shown that in aqueous acidic media, stepped surfaces exhibit higher activity for oxygen reduction when compared to the basal planes [24,25]. We conclude that the high activity usually observed for {110} is due to the predominantly disordered (1 × 2) structure being present. Imperfections in the (1 × 1) phase act to enhance electrocatalytic activity. We ascribe the mechanism by which this occurs to the break-up of a long range OH ordered structure present at the surface of Pt{110}-(1 × 1) which acts to prevent O₂ adsorbing, a model postulated originally by Markovic et al. for Pt{111} in perchloric acid [36].

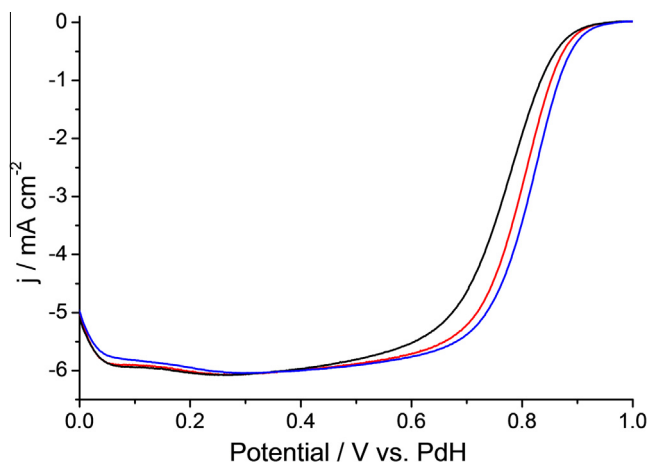


Fig. 5. ORR data of Pt{110}-(1 × 1), black, hydrogen-cooled Pt{110}, red and nitrogen-cooled Pt{110}, blue in O₂ saturated 0.1 mol dm⁻³ HClO₄. A hanging meniscus rotating disc electrode configuration with sweep rate = 30 mV s⁻¹, 1 atm O₂ pressure and 1600 rpm rotation rate was utilised. The first positive going sweep is reported here. (For interpretation of the references to colour in this figure legend, the reader is referred to the web version of this article.)

4. Conclusions

The (1 × 1) and disordered (1 × 2) surface atomic arrangements of Pt{110} have been compared using their voltammetry in sulphuric acid, perchloric acid and sodium hydroxide. The voltammetry in sulphuric acid showed similarities to that reported by Kolb et al. and Markovic et al. For the first time, the voltammetry of the Pt{110}-(1 × 1) surface has been reported in perchloric acid and sodium hydroxide. Perchloric acid voltammetry of the (1 × 1) surface exhibited 6 peaks in the potential range 0–0.3 V in stark contrast to the two broad peaks observed in the voltammetry of the disordered (1 × 2) surface. The (1 × 1) surface also exhibits a singular, large oxide electroadsorption peak at 0.95 V and almost zero current associated with electroadsorption at defects. This implies an atomically perfect Pt{110}-(1 × 1) surface. In contrast, the emergence of OH electroadsorption peaks close to 0.75 V we ascribe to the generation of Pt{110}-(1 × 2) phases in which highly uncoordinated surface Pt atoms act as nucleation centres for oxide formation. It is concluded that the Pt{110} surface exhibits a mixed H_{ads}/OH_{ads} adlayer in the 0.09–0.2 V potential range and that the large number of peaks occurring are due to new adlayer structures, with differing hydrogen/OH ratios becoming stable at different potentials.

The activity of the Pt{110}-(1 × 1) surface for oxygen reduction was also tested and was found to be approximately 30–40 mV less active than any of the disordered (1 × 2) surfaces studied when $E_{1/2}$ values for ORR are compared.

Acknowledgement

GAA acknowledges the financial support of the EPSRC towards a studentship for AB (grant number EP/J500197/1).

References

- [1] N. Tian, Z. Zhou, S. Sun, J. Phys. Chem. C 112 (2008) 19801–19817.
- [2] M.A. Van Hove, R.J. Koestner, P.C. Stair, J.P. Bibérian, L.L. Kesmodel, I. Bartoš, G.A. Somorjai, Surf. Sci. 103 (1981) 189–217.
- [3] M.A. Van Hove, R.J. Koestner, P.C. Stair, J.P. Bibérian, L.L. Kesmodel, I. Bartoš, G.A. Somorjai, Surf. Sci. 103 (1981) 218–238.
- [4] A.R. Sandy, S.G.J. Mochrie, D.M. Zehner, G. Grübel, K.G. Huang, D. Gibbs, Phys. Rev. Lett. 68 (1992) 2192–2195.
- [5] G. Grübel, K.G. Huang, D. Gibbs, D.M. Zehner, A.R. Sandy, S.G.J. Mochrie, Phys. Rev. B 48 (1993) 18119–18139.
- [6] M. Bott, M. Hohage, T. Michely, G. Comsa, Phys. Rev. Lett. 70 (1993) 1489–1492.
- [7] M. Hohage, T. Michely, G. Comsa, Surf. Sci. 337 (1995) 249–267.
- [8] A. Al-Akl, G.A. Attard, R. Price, B. Timothy, J. Electroanal. Chem. 467 (1999) 60–66.
- [9] M.S. Zei, N. Batina, D.M. Kolb, Surf. Sci. 306 (1994) L519–L528.
- [10] F.G. Will, J. Electrochem. Soc. 112 (1965) 451–455.
- [11] J. Clavilier, R. Faure, G. Guinet, R. Durand, J. Electroanal. Chem. 107 (1980) 205–209.
- [12] J. Clavilier, J. Electroanal. Chem. 107 (1980) 211–216.
- [13] L.A. Kibler, A. Cuesta, M. Kleinert, D.M. Kolb, J. Electroanal. Chem. 484 (2000) 73–82.
- [14] A. Al-Akl, G. Attard, R. Price, B. Timothy, J. Chem. Soc., Faraday Trans. 91 (1995) 3585–3591.
- [15] N.M. Marković, B.N. Grgur, C.A. Lucas, P.N. Ross, Surf. Sci. 384 (1997) L805–L814.
- [16] R. Michaelis, D.M. Kolb, J. Electroanal. Chem. 328 (1992) 341–348.
- [17] P. Hofmann, S.R. Bare, D.A. King, Surf. Sci. 117 (1982) 245–256.
- [18] J. Souza-Garcia, V. Climent, J.M. Feliu, Electrochem. Commun. 11 (2009) 1515–1518.
- [19] J. Souza-Garcia, C.A. Angelucci, V. Climent, J.M. Feliu, Electrochem. Commun. 34 (2013) 291–294.
- [20] A.M. Bittner, J. Wintterlin, G. Ertl, J. Electroanal. Chem. 388 (1995) 225–231.
- [21] P. Rodríguez, G. García, E. Herrero, J.M. Feliu, M.T.M. Koper, Electroanalysis 2 (2011) 242–253.
- [22] J. Perez, H.M. Villullas, E.R. Gonzalez, J. Electroanal. Chem. 435 (1997) 179–187.
- [23] N.M. Marković, R.R. Adzic, B.D. Cahan, E.B. Yeager, J. Electroanal. Chem. 377 (1994) 249–259.
- [24] M.D. Macia, J.M. Campina, E. Herrero, J.M. Feliu, J. Electroanal. Chem. 564 (2004) 141–150.
- [25] A. Kuzume, E. Herrero, J.M. Feliu, J. Electroanal. Chem. 599 (2007) 333–343.
- [26] H. Tanaka, Y. Nagahara, S. Sugawara, K. Shinohara, M. Nakamura, N. Hoshi, Electroanalysis 5 (2014) 354–360.
- [27] S. Kondo, M. Nakamura, N. Maki, N. Hoshi, J. Phys. Chem. C 113 (2009) 12625–12628.
- [28] N. Marković, M. Hanson, G. McDougall, E. Yeager, J. Electroanal. Chem. Interfacial Electrochem. 214 (1986) 555–566.
- [29] B.D. Cahan, H.M. Villullas, J. Electroanal. Chem. Interfacial Electrochem. 307 (1991) 263–268.
- [30] N.M. Marković, B.N. Grgur, P.N. Ross, J. Phys. Chem. B 101 (1997) 5405–5413.
- [31] V. Climent, G.A. Attard, J.M. Feliu, J. Electroanal. Chem. 532 (2002) 67–74.
- [32] M.T.M. Koper, J.J. Lukkien, J. Electroanal. Chem. 485 (2000) 161–165.
- [33] N. Garcia-Araez, V. Climent, J.M. Feliu, J. Electroanal. Chem. 649 (2010) 69–82.
- [34] R. Rizo, E. Sitta, E. Herrero, V. Climent, J.M. Feliu, Electrochim. Acta (2015).
- [35] N. Furuya, M. Shibata, J. Electroanal. Chem. 467 (1999) 85–91.
- [36] J.X. Wang, N.M. Marković, R.R. Adzic, J. Phys. Chem. B 108 (2004) 4127–4133.